
GENERAL EXPERIMENTAL
TECHNIQUES

A Method for Investigating Nanosecond Processes in Micropinch Discharge Plasma

A. N. Dolgov^{a,*}, N. A. Klyachin^b, and D. E. Prokhorovich^{a,b}

^a *Dukhov All-Russia Research Institute of Automatics, Moscow, 127055 Russia*

^b *National Research Nuclear University MEPhI, Moscow, 115409 Russia*

**e-mail: alnikdolgov@mail.ru*

Received December 9, 2021; revised February 5, 2022; accepted February 18, 2022

Abstract—The technique is described and the results of studies of the spatial structure and dynamics of X-ray sources in the plasma of a micropinch discharge are presented. The applied technique made it possible to temporarily link the process of electron acceleration in a quasi-static electric field of a resistive nature to the process of forming a microstretch in a Z-pinch in a medium of heavy elements with a nanosecond time resolution.

DOI: 10.1134/S0020441222040091

An important task, which has to be constantly solved in a wide variety of conditions using various methods of plasma diagnostics when studying pulsed electrical discharges is the study of the spatial structure of plasma and the dynamics of processes occurring in the discharge plasma with a high time resolution [1–5].

This paper describes a method that allows one to somehow shift in time the process of the influence of an electric field on the conditions of the ordered movement of electric charges in plasma relative to the process of changing the spatial structure of the discharge plasma over time due to the interaction of the current flow in plasma and the magnetic field induced by it, which is known as pinching. This makes it possible to better understand the cause-and-effect relations or, at least, the sequence of the occurring phenomena.

This research was carried out on an experimental bench with an electric-discharge device of the high-current low-inductance vacuum-spark type, whose design and parameters were described repeatedly [2–5]. The relative simplicity of the design and operating conditions, compactness, and, at the same time, the ability to obtain high-temperature dense plasma make this device a convenient tool for conducting fundamental research, e.g., modeling processes that occur in inaccessible astrophysical objects, or for use in extremely expensive laboratory devices, which are intended to solve the problem of controlled thermonuclear fusion. In addition, the device can be used to solve applied problems, e.g., as a simulator of natural or artificial sources of high-power X-ray and ultraviolet radiation pulses or directly as a source of short-wavelength radiation in lithography technology [2, 4, 6].

The discharge was performed in a vacuum chamber that was evacuated to a vacuum of no worse than 10^{-2} Pa. The working substance of the discharge is ionized vapors of the electrode material, mainly the anode. A battery of low-inductance high-voltage capacitors is the pulsed current source. The electrodes of the discharge device are made of iron (low-carbon steel). A rod with a diameter of 3 mm and a length of 15 mm, which was pointed as a cone at the end that faced the cathode, was used as the anode. The cathode has the shape of a cylinder, whose axis of symmetry coincides with the discharge axis and the diameter is 20 mm. The cathode faces the anode with its flat base and has a through hole on the axis of symmetry; a plug or a pointed tip, which faces the anode, can be screwed into this hole. The distance between the electrodes is 5 mm. The electrodes are combined in a single circuit with the capacitor bank by means of coaxial current leads that extend beyond the vacuum chamber and are separated by a nylon insulator; the capacitor bank was connected using a system of parallel coaxial cables. The discharge was initiated by the injection of fore-plasma from four auxiliary erosive-type low-current sources, which were located around the discharge axis, into the interelectrode space (Fig. 1).

The amplitude of the first current pulse in the discharge, near whose maximum short-wave electromagnetic radiation sources were formed, was 100 kA at a charging voltage of the capacitor bank of 10 kV. The time of reaching the maximum current from the moment of the registered start of the current flow between the cathode and anode was 1.0 μ s.

The capacitance of the cables that were used to connect the electrode assembly (current leads and

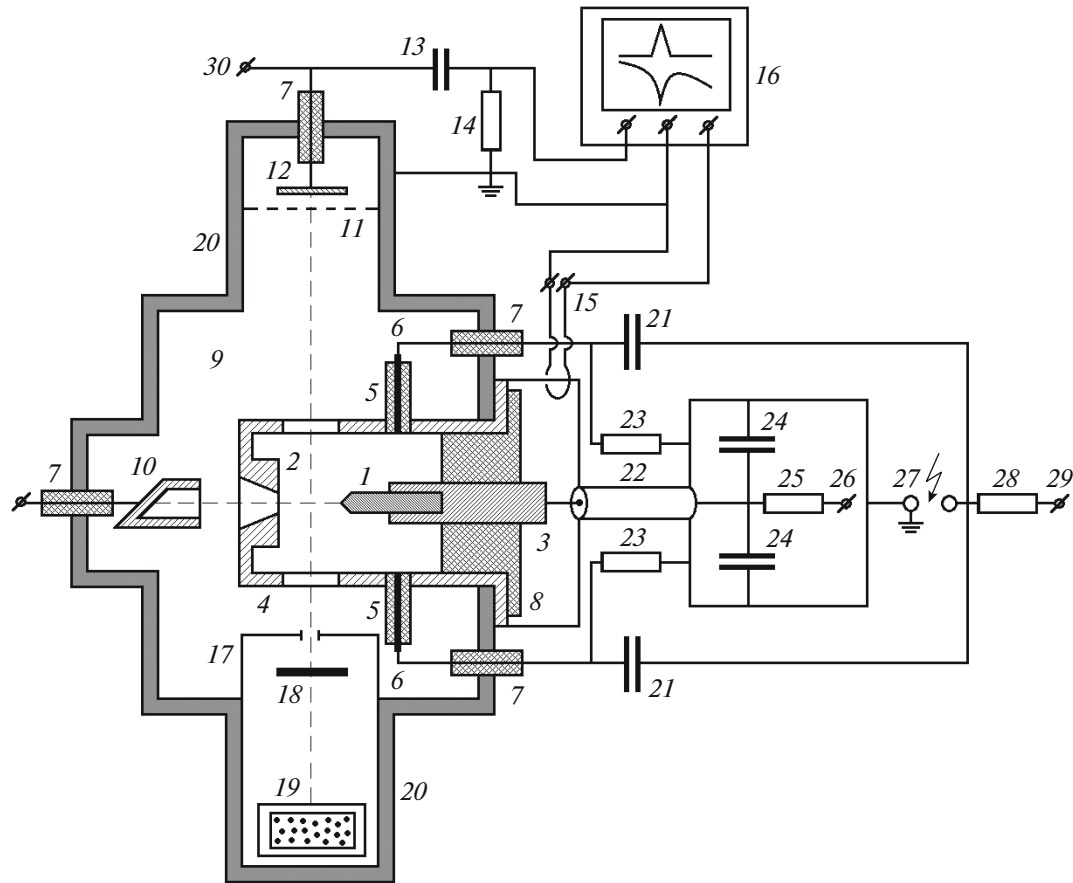


Fig. 1. Schematic diagram of the experiment: (1) inner electrode, (2) outer electrode, (3) inner current lead, (4) outer current lead, (5) dielectric bushing, (6) igniter electrode, (7) feedthrough insulator, (8) blocking insulator, (9) vacuum chamber, (10) charged-particle collector with a biased potential, (11) anode of the vacuum biplanar photodiode, (12) cathode of the vacuum biplanar photodiode, (13) blocking capacitor, (14) load resistance, (15) Rogowski coil, (16) oscilloscope, (17) objective lens of the pinhole camera, (18) absorbing thin-film filter, (19) photographic detector of X rays, (20) auxiliary vacuum chamber, (21) capacitor bank in the igniter circuit, (22) forming cable line, (23) shunting resistor, (24) capacitor bank in the main-discharge circuit, (25) ballast resistor, (26) connection of the high-voltage stabilized voltage source for charging the capacitor bank in the main-discharge circuit, (27) triggered spark gap, (28) limiting resistor, (29) connection of the high-voltage stabilized voltage source for charging the capacitor bank in the igniter circuit, and (30) connection of the high-voltage stabilized voltage source for supplying the planar-photodiode circuit.

electrodes) to the capacitor bank did not exceed 0.04% of the capacitor-bank capacitance. According to estimates, the capacitance of the electrode assembly was much lower than the capacitance of the cables. Thus, the parameters of the current that flows when the interelectrode gap is closed by the discharge plasma, i.e., its period and, with good accuracy, the amplitude of the first pulse, were determined by the inductance of the circuit and the capacitance of the capacitor bank since the ohmic resistance of the circuit is much lower than its characteristic resistance.

In essence, we can consider the system of coaxial cables as a forming line with the distributed capacitance and inductance along which an electromagnetic wave propagates at the velocity

$$V_{\text{wave}} = c/(\epsilon)^{1/2}, \quad (1)$$

where c is the velocity of light in vacuum and ϵ is the permittivity of the insulator that separates the core and the braid in the cable ($\epsilon = 2.3$ for polyethylene). In our case, $V_{\text{wave}} = 2 \times 10^8$ m/s.

The discharge mode was monitored using a Rogowski coil in the current-transformer mode and a vacuum biplanar photodiode that records the dynamics of vacuum UV radiation and discharge-emitted soft X rays. The evidence of the pinching mode was the appearance of a dip in the discharge-current curve (the so-called “singularity”) near its maximum. Registering a pulse of vacuum UV radiation and soft X-ray radiation, which is synchronous with the “singularity” of a signal from the Rogowski coil, indicated the development of the pinching process up to the formation of a micropinch, i.e., an object with micron dimensions.

The design basis of the photodiode is a vacuum high-frequency electrical connector of the VRG type. An aluminum, 10-mm diameter photocathode is attached on a tight fit to the central current lead of the connector. A copper bushing is screwed onto the external current lead of the connector, on which a mesh anode with a cell size of 0.5 mm and a transmission of 0.95 is fixed. The distance between the anode and cathode is 1 mm. A negative potential of 0.8–1.5 kV is supplied to the cathode from a high-voltage stabilized voltage source. A capacitance of 2200 pF separates the recording equipment (an oscilloscope) from the high-voltage power-supply circuit. The radiation that is incident on the photocathode initiates a current of photoelectrons that are accelerated by an electric field applied to the cathode, while the induced current flows through a circuit formed by a blocking capacitor and a 50- Ω load resistance. A registered voltage pulse is formed across the load resistance.

The spatial structure of X-ray sources in the discharge was studied using a pinhole camera, which was placed outside the vacuum chamber. The radiation was removed from the vacuum chamber through a beryllium window with a thickness of 100 μm in a thick-walled metal flange. The image-forming lens was a 0.2-mm-diameter hole made in 0.2-mm-thick lead foil, which served as an absorbing diaphragm. The image was recorded on a medical X-ray photographic film, which was protected against illumination in the visible spectrum by a screen permeable to X rays with a wavelength of $\lambda < 0.3$ nm and impermeable to optical radiation. The images that were obtained with a pinhole camera simultaneously allowed us to control the nature of the discharge. The development of the pinching process up to the formation of a micron-size microstretch of the plasma current channel in the discharge, i.e., the formation of a micropinch (its size is much smaller than the aperture diameter in the diaphragm), led to the appearance of a characteristic bright image of the aperture in the diaphragm, which is often called a “hot spot” image on an obscurogram.

The registration of signals from the Rogovsky coil and the vacuum biplanar photodiode showed that the development of the pinching process up to the formation of a micropinch is steadily performed in a discharge that is realized on the experimental bench described above (during the first quarter of the discharge-current flow period, or rather, near the moment when the maximum current is reached, i.e., obviously until the electrodes are reversed). However, this circumstance was established and confirmed previously by us many times, including with the help of additional diagnostic tools [1–4].

Figure 2 shows an X-ray obscurogram of the interelectrode gap that was obtained under the following conditions: at the time of the discharge initiation, the anode served as the internal electrode, while the cathode served as the outer electrode, and the forming-line



Fig. 2. X-ray obscurogram of the interelectrode gap recorded under the following conditions: at the time of the discharge initiation, the internal electrode is the anode, the outer electrode is the cathode, and the length of the forming line is 1 m.

length was 1 m. The formation of a micropinch is observed, which is recorded as a “hot spot,” i.e., an almost point source of X rays. In addition, a glow is observed in the above-mentioned X-ray spectrum range of the inner-electrode surface and peripheral plasma outside of the microstretch region in the space between the micropinch and the inner electrode. It can be noted that a relatively bright and local X-ray source with a size of ~ 500 μm is present on the inner-electrode surface in the region of the surface intersection with the discharge axis.

Figure 3 shows an X-ray obscurogram that was obtained with the same polarity of the electrodes but with a length of the forming line of 2 m. In this case, in addition to the glow of the inner-electrode surface, the micropinch, and the peripheral plasma, a glow of the outer-electrode surface is observed.

Finally, Figs. 4 and 5 show X-ray obscurograms that were obtained when the length of the forming line was increased to 3 m. At the time of the discharge initiation, the anode served as the inner electrode, while the cathode served as the outer electrode (the outer electrode is flat in Fig. 4, while there is a pointed protrusion (tip) on the flat surface of the outer electrode in Fig. 5). A similar image is formed when the length of the forming line is 1 m and in the case when the inner and outer electrodes are the cathode and anode, respectively. There is a glow from the micropinch, peripheral plasma that runs into the outer electrode, and the surface of the outer electrode itself; however, no glow of the inner electrode and plasma that is located between the micropinch and outer electrode is observed.

The recorded time-resolved spectrum of X-ray bremsstrahlung demonstrates that the formation of a micropinch in the microstretch region is accompanied by the development of accelerating processes, i.e., the deviation of the electron distribution from the Max-

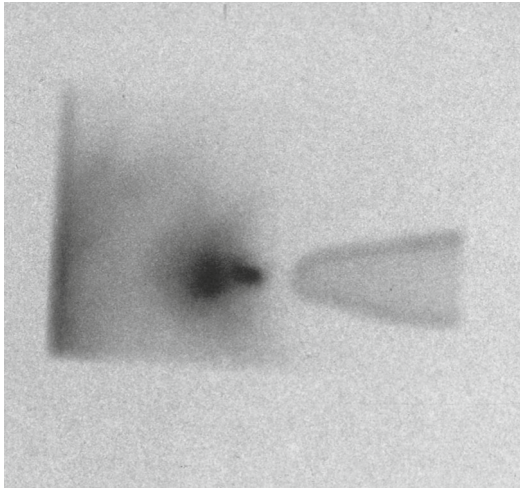


Fig. 3. X-ray obscurogram of the interelectrode gap recorded under the following conditions: at the time of the discharge initiation, the internal electrode is the anode, the outer electrode is the cathode, and the length of the forming line is 2 m.

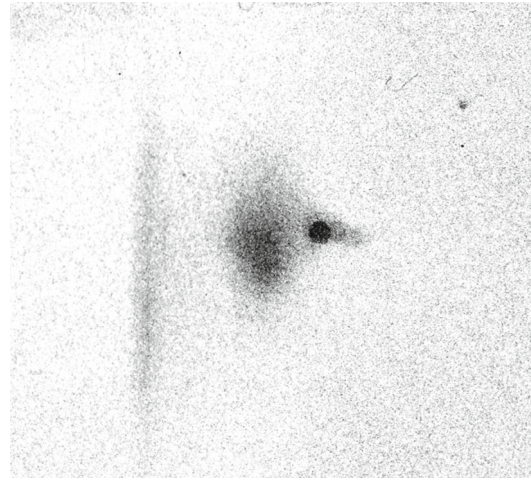


Fig. 4. X-ray obscurogram of the interelectrode gap recorded under the following conditions: at the time of the discharge initiation, the internal electrode is the anode, the outer flat electrode is the cathode, and the length of the forming line is 3 m.

wellian one under the action of a quasi-static electric field of a resistive nature becomes increasingly noticeable. According to experimental data, the duration of the development of accelerating processes is 30 ns [2]. The formation of a micropinch region in a pinching discharge in a medium of heavy elements with currents flowing through the microstretch region, which exceed the critical value (~ 50 kA for iron plasma), occurs in two stages. Initially, as a result of the outflow of matter from the microstretch, the first or magnetohydrodynamic compression occurs to a radius of $\sim 10^{-4}$ m. Then, approximately 10^{-8} – 10^{-7} s later, a second or radiative compression to a radius of $\sim 10^{-6}$ m occurs within a time of $\sim 10^{-10}$ s, which is caused by radiant energy losses [1, 2, 4, 7, 8]. It should be noted that the recorded duration of the development of the acceleration processes significantly exceeds the duration of the second compression and fits into the duration of the time interval between the first and second compressions. An approximate calculation shows that upon completion of the first compression, the electron current velocity turns out to be much higher than the ion-sound velocity, which is approximately equal to the average thermal velocity of ions. Under these conditions, plasma oscillations in the microstretch region must intensify and the ohmic resistance of plasma must increase due to the electron scattering by them; this will lead to plasma heating, an increase in the multiplicity of ions, an increase in the level of radiative energy losses, and an increase in the potential drop at a slight current change due to the significant inductance of the circuit [9]. The forming line, whose capacitance at a length of 3 m is $C \approx 10^{-9}$ F, shunts the discharge and decelerates the development of accelerating processes that are associated with an increase in

the ohmic resistance of plasma and, as a consequence, with an increase in the potential drop in the microstretch region.

The authors of [10] have shown that the pinch resistance is also maximized at the moment of reaching the local compression maximum on the time scale. The resistance of the microstretch at the moment of the maximum compression under conditions of low radiation energy losses is determined only by the plasma temperature in the microstretch [11]:

$$R_{\text{pinch}} = (5\mu_0 / (8\pi)) [5(Z + 1)kT_e / (3M_i)]^{1/2}, \quad (2)$$

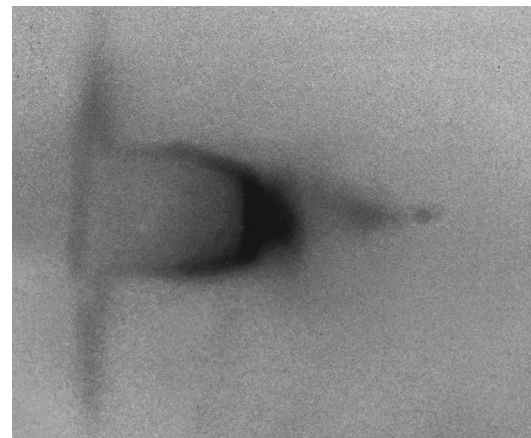


Fig. 5. X-ray obscurogram of the interelectrode gap recorded under the following conditions: at the time of the discharge initiation, the internal electrode is the anode; the outer flat electrode, at whose center there is a metallic protrusion, is the cathode; and the length of the forming line is 3 m.

where μ_0 is the magnetic constant, Z is the average ionization level of atomic particles, k is the Boltzmann constant, T_e is the electron temperature of plasma in the microstretch, and M_i is the ion mass.

In the case of the predominant influence of radiation losses on the pinch dynamics, the micropinch resistance is determined from the balance of the Joule heat release power and the radiation power:

$$R_{\text{pinch}}^* = P_{\text{rad}}/I^2, \quad (3)$$

where P_{rad} is the power of the radiant energy losses by the pinch plasma, and I is the discharge current.

The resistance R_{pinch}^* may be significantly higher than the resistance possessed by the microstretch region in the case of losses due only to the plasma outflow. Indeed, if we estimate the ohmic resistance for plasma within the framework of the above model, we obtain the following results. At the stage of the existence of a quasi-static plasma column that precedes the development of microstretch instability, we obtain $R_{\text{pinch}}^{(0)} = 2 \times 10^{-2} \Omega$ without taking the energy loss by radiation into account and $R_{\text{pinch}}^{*(0)} = 2 \times 10^{-2} \Omega$ taking the energy loss by radiation into account. When the first compression is over, we obtain $R_{\text{pinch}}^{(1)} = 2 \times 10^{-2} \Omega$ without taking the energy loss by radiation into account and $R_{\text{pinch}}^{*(1)} = 10^{-1} \Omega$ with account of the energy loss by radiation. When the second compression is over, we obtain $R_{\text{pinch}}^{(2)} = 3 \times 10^{-2} \Omega$ and $R_{\text{pinch}}^{*(2)} = 10 \Omega$, respectively. For the current $I = 10^5$ A, the voltage of the resistive electric field in the micropinch reaches $\sim 10^4$ V in the first and $\sim 10^6$ V in the second compression [11].

The analysis of the experimentally observed spatial structure of X-ray sources (see Figs. 2–5), which is based on the above experimental data and the results of theoretical modeling, suggests the following conclusions. Apparently, in the interval between the first and second compressions, the charging of the forming line and a delay in the development of accelerating processes in plasma occur for a period of ~ 10 , 20, and 30 ns depending on the length of the forming line. The delay in the appearance of an electric field of resistive nature with respect to the dynamics of the plasma in the microstretch region changes the conditions for the propagation of accelerated electrons. They can be associated, e.g., with the formation of a directed plasma stream moving along the discharge axis. There is experimental evidence that the micropinch formation region moves along the discharge axis from the inner electrode to the outer one and, in addition, the axial stream of plasma that outflows from the microstretch region has a noticeably higher velocity in the direction of the outer electrode than in the opposite direction (in the direction of the inner electrode) [12–14]. The rate of the plasma outflow from the microstretch

region in the direction of the outer electrode may reach a Mach number of 3–4 [11]. It can be assumed that a plasma stream is formed at the stage of the transition from the first to the second compression, which carries away “hot” electrons, i.e., electrons that are accelerated in an electric field of resistive nature, which are magnetized in the direction from the inner to the outer electrode, regardless of the polarity of the electrodes, unless the acceleration process is delayed until the moment when the possibility of runaway of electrons in the paraxial region of the minimum magnetic field disappears. Within the framework of the above assumptions, we can give the following explanation for the discharge images that were obtained using an X-ray pinhole camera. In Fig. 2 that corresponds to a situation with a delay in the acceleration of electrons by ~ 10 ns (the length of the forming line is 1 m), we observe evidence of the electrons runaway in the paraxial region: this is a local X-ray source at the top of the inner electrode [15]. Such an object is no longer observed in Fig. 3; however, at the same time, as a result of the emission of X-ray radiation from the discharge plasma, a stream of “hot” electrons and plasma that propagates in the direction of the outer electrode reveals itself. The plasma stream in the direction of the inner electrode does not reveal itself, although we can observe traces of the bombardment of the inner electrode with “hot” electrons by its glow in the X-ray spectral range. Consequently, the axial plasma stream in the direction of the outer electrode already exists ~ 20 ns (the length of the forming line is 2 m) after the activation of the electron acceleration mechanism, and the runaway of electrons in the paraxial region becomes impossible. Probably, the latter circumstance indicates that the runaway of electrons in the paraxial region is prevented by the excitation of plasma oscillations. The images in Figs. 4 and 5 (the delay of the electron acceleration process is ~ 30 ns with a length of the forming line of 3 m) demonstrate that the effect of the plasma stream on “hot” electrons excludes their ingress to the inner electrode.

The study of the discharge-plasma temperature dynamics, which is based on measurements with a sufficiently high time resolution of the spectral characteristics of bremsstrahlung X-rays of discharge plasma, shows that the electron energy distribution can be represented in a two-temperature approximation at the stage of a transition from the first to the second compression. In other words, there are two components of the electron component in the discharge plasma that can be conditionally called cold and hot components. The temperature of the hot component at the stage of the transition from the first to the second compression reaches ~ 10 keV, while the temperature of the cold component is ~ 2 keV [2]. The electrical conductivity of plasma is determined by the hot-component temperature and has the following value [16]:

$$\sigma = 2 \times 10^{-2} T_e^{3/2} / (\Lambda Z) \approx 3 \times 10^8 \Omega^{-1} \text{ m}^{-1}, \quad (4)$$

where $T_e \approx 10 \text{ keV} \approx 10^8 \text{ K}$ is the maximum temperature of the hot electron component, $\Lambda \approx 10$ is the Coulomb logarithm, and $Z \approx 10$ is the average ion charge.

For a duration of the considered stage of $\tau \leq 3 \times 10^{-8} \text{ s}$ and a typical value of the plasma displacement $s \approx 10^{-4} \text{ m}$, which corresponds to a value of the order of the microstretch radius in the first compression, the following relationship is valid:

$$s \gg [\tau/(\mu_0 \sigma)]^{1/2}, \quad (5)$$

which is the condition for the magnetic-field freezing-in. Thus, the formation of a directed plasma stream in the microstretch may lead to a distortion of the pattern of the magnetic-field lines of force that are entrained by the plasma stream. As can be easily seen, accelerated electrons with energies of $\sim 10^5 \text{ eV}$ are magnetized (except for the paraxial region [16]):

$$r_L \approx 10^{-5} \text{ m} \ll s \approx 10^{-4} \text{ m}, \quad \lambda \approx 10^{-1} \text{ m}. \quad (6)$$

Here, r_L is the Larmor radius of a fast electron; $\lambda \approx v_e \tau_{ei}$ is the free path of an electron in plasma, where v_e and τ_{ei} are, respectively, the velocity and the mean time between collisions of electrons with ions; the latter quantity is estimated as [17]

$$\tau_{ei} \approx 4.5 \times 10^{-2} T_e^{3/2} / (Z n_e), \quad (7)$$

where the average kinetic energy of accelerated electrons is taken for $T_e \approx 10^5 \text{ eV} \approx 10^9 \text{ K}$; $Z \approx 10$; $n_e \approx 10^{20} \text{ cm}^{-3}$ is the electron plasma concentration after the first compression. The entrainment of magnetic field lines by the plasma stream, in turn, will lead to the entrainment of magnetized accelerated high-energy electrons by the plasma stream.

At what stage of the microstretch development does the formation of an axial plasma stream occur in the direction of the outer electrode? Judging by the images on the obtained X-ray obscurograms, the formation of the axial plasma stream begins in the time interval between the first and second compressions in $\sim 10 \text{ ns}$ or a little more after the activation of the acceleration mechanism for electrons in an electric field of a resistive nature. A stream is formed $\sim 30 \text{ ns}$ after the acceleration mechanism is enabled. According to measurements performed on the same experimental bench, the duration of the electron acceleration process is $\sim 30 \text{ ns}$ [2]. It can be concluded that the formation of a plasma stream in the direction of the outer electrode begins after heating the plasma in the microstretch, which is formed in the first compression, to a temperature at which the transition to the second (radiative) compression becomes possible. Probably, in the compression process that proceeds at an increasing speed, the microstretch slides along the discharge axis in the direction from the inner to the outer electrode and serves as a piston that entrains plasma in the same direction in the current channel.

Thus, the use of a combined current source in the form of a capacitor bank and a variable-length forming

line, which are connected in parallel, made it possible to detect a phenomenon that was not previously described in the literature. When using a forming line of sufficient length, a flow of high-energy electrons with an energy of $\geq 10^4 \text{ eV}$ per particle—which propagate in the direction of the outer electrode, regardless of the polarity of the electrodes—is observed. Based on the results of the performed experiments and numerical estimates, the authors conclude that the presence of the forming line delays the acceleration of electrons in a quasi-static electric field of a resistive nature in the microstretch region at the stage of a transition to radiative compression and leads to the advanced formation of an anisotropic axial plasma stream. The propagation direction of the high-energy electron flow is determined by the freezing of the magnetic-field lines in the plasma stream and magnetization of electrons accelerated to high energies.

The images obtained by visualizing the spatial structure of the discharge plasma that emits in the X-ray range convincingly demonstrate that a paraxial plasma stream, which is directed from the inner electrode to the outer one, is formed during pinching.

Another conclusion that can be drawn from the obtained results is that the development of accelerating processes in an electric field of a resistive nature begins even before the second compression occurs, contrary to the established point of view. The conventional version of the mechanism for the formation of a fast electron flow in a micropinch discharge assumes their acceleration in an electric field, which is generated due to the development of an abnormal plasma resistance upon a microstretch break as a result of the radiative compression [18–20]. Consequently, the authors' version about the possibility of a Coulomb explosion in a micropinch at the stage of the transition from the first to second compression, i.e., before the radiative compression [21], is confirmed.

OPEN ACCESS

This article is licensed under a Creative Commons Attribution 4.0 International License, which permits use, sharing, adaptation, distribution and reproduction in any medium or format, as long as you give appropriate credit to the original author(s) and the source, provide a link to the Creative Commons license, and indicate if changes were made. The images or other third party material in this article are included in the article's Creative Commons license, unless indicated otherwise in a credit line to the material. If material is not included in the article's Creative Commons license and your intended use is not permitted by statutory regulation or exceeds the permitted use, you will need to obtain permission directly from the copyright holder. To view a copy of this license, visit <http://creativecommons.org/licenses/by/4.0/>.

REFERENCES

1. Veretennikov, V.A., Polukhin, S.N., Semenov, O.G., and Sidel'nikov, Yu.V., *Fiz. Plazmy* (Moscow), 1981, vol. 7, no. 6, p. 1199.
2. Averkiev, V.V., Dolgov, A.N., Lyapidevskii, V.K., Savelov, A.S., and Salakhutdinov, G.Kh., *Fiz. Plazmy* (Moscow), 1992, vol. 18, no. 6, p. 724.
3. Gulin, M.A., Dolgov, A.N., Kirichenko, N.N., and Savelov, A.S., *Zh. Eksp. Teor. Fiz.*, 1995, vol. 108, no. 10, p. 1309.
4. Dolgov, A.N., Lyapidevskii, V.K., Prokhorovich, D.E., Savelov, A.S., and Salakhutdinov, G.Kh., *Plasma Phys. Rep.*, 2005, vol. 31, no. 2, p. 167.
5. Dolgov, A.N., Zemchenkova, N.V., Klyachin, N.A., and Prokhorovich, D.E., *Prikl. Fiz.*, 2012, no. 1, p. 68.
6. Veretennikov, V.A., Dolgov, A.N., Kantsyrev, V.L., Sagalovskaya, O.V., and Semenov, O.G., *Poverkhnost*, 1984, no. 4, p. 115.
7. Blinnikov, S.I. and Imshennik, V.S., *Fiz. Plazmy* (Moscow), 1982, vol. 8, no. 1, p. 193.
8. Vikhrev, V.V., Ivanov, V.V., Koshelev, K.N., and Sidel'nikov, Yu.V., *Dokl. Akad. Nauk SSSR*, 1982, vol. 282, p. 1361.
9. Vikhrev, V.V., Ivanov, V.V., and Koshelev, K.N., *Preprint of Kurchatov Institute of Atomic Energy*, Moscow, 1980, no. 3359/6.
10. Vikhrev, V.V., Ivanov, V.V., and Rozanova, G.A., *Nucl. Fusion*, 1993, vol. 33, no. 2, p. 311.
11. Dolgov, A.N. and Vikhrev, V.V., *Plasma Phys. Rep.*, 2005, vol. 31, no. 3, p. 259.
12. Lee, T.N., *Ann. N. Y. Acad. Sci.*, 1975, vol. 251, p. 112
13. Afonin, V.I., *Fiz. Plazmy* (Moscow), 1995, vol. 21, no. 7, p. 648.
14. Dolgov, A.N., *Plasma Phys. Rep.*, 2005, vol. 31, no. 6, p. 493.
15. Dolgov, A.N., Zemchenkova, N.V., Klyachin, N.A., and Prokhorovich, D.E., *Plasma Phys. Rep.*, 2011, vol. 37, no. 3, p. 203.
16. Kozlov, N.P., *Osnovy fiziki plazmy* (Fundamentals for Plasma Physics), Moscow: Bauman Moscow State Technical Univ., 1997.
17. Zhdanov, S.K., Kurnaev, V.A., Romanovskii, M.K., and Tsvetkov, I.V., *Osnovy fizicheskikh protsessov v plazme i plazmennykh ustanovkakh* (Fundamentals for Physical Processes in Plasma and Plasma Plants), Kurnaev, V.A., Ed., Moscow: Moscow Engineering Physics Institute, 2007.
18. Fukai, J. and Clothiaux, E.J., *Phys. Rev. Lett.*, 1975, vols. 3–4, no. 4, p. 863.
19. Korop, E.D., Meierovich, B.E., Sidel'nikov, Yu.V., and Sukhorukov, S.T., *Usp. Fiz. Nauk*, 1979, vol. 129, no. 1, p. 87.
20. Shelkovenko, T.A., Pikuz, S.A., Mingaleev, A.R., Agafonov, A.V., Romanova, V.M., Ter-Oganes'yan, A.E., Tkachenko, S.I., Blesner, I.S., Mitchell, M.D., Chandler, K.M., Kussi, B.R., and Hammer, D.A., *Plasma Phys. Rep.*, 2008, vol. 34, no. 9, p. 754.
21. Dolgov, A.N., Klyachin, N.A., and Prokhorovich, D.E., *Prikl. Fiz.*, 2019, no. 3, p. 10.

Translated by A. Seferov